Optical and IR Interferometry from Ground and Space
ASP Conference Series, Vol. 3 × 10^8, 1999
S.C. Unwin, and R.V. Stachnick, eds.

Sensitivity of the TPF Interferometer for Planet Detection

C.A. Beichman and T. Velusamy

Jet Propulsion Laboratory, California Institute of Technology, Pasadena, CA 91109

Abstract. The Terrestrial Planet Finder (TPF) offers the prospect of revolutionizing humanity's perception of its own place in the Universe by identifying habitable and possibly even life-bearing planets orbiting other stars. TPF will be able to find planets that are like the Earth in essential respects: warm, with water and an oxygen-containing atmosphere. This paper introduces some of the issues that define the sensitivity of TPF for planet detection. TPF will also be able to image astrophysical sources with sub-milli-arcsecond resolution, but that topic is beyond the scope of this paper. The major conclusion of this paper is that a nulling interferometer operating at 1 AU with four 3.5-m telescopes can detect and characterize Earth-like planets as far away as 15 pc. A smaller system using ~2.5-m apertures could still detect Earth-like planets but would not be able to search for signs of life, such as ozone, in any but the nearest planetary systems.

1. Introduction

A typical star is more than a billion (in the optical) to a million (in the thermal infrared) times brighter than the planet, making the planet undetectable in the star's glare without special efforts to cancel out the starlight (Figure 1). This cancellation must operate at the 0.1 arcsec angular separation presented by a 1 AU orbit around a star 10 pc away. Scientific reasons such as the existence of strong, broad spectral features (CO_2, H_2O, O_3 and possibly CH_4) and technical reasons such as the thousand-fold more favorable contrast ratio favor searching for planets in the mid-infrared. These arguments are summarized along with a complete description of the present TPF concept in a recently published report TPF: *The Terrestrial Planet Finder* (Beichman, Woolf, and Lindensmith 1999).

Bracewell and MacPhie (1979) were the first to suggest that a space-based infrared interferometer could suppress the starlight by pointing a null in an interference pattern onto the star while simultaneously detecting the planet through an adjacent bright fringe. To allow the signal from the planet to be distinguished from noise and background sources, they further proposed rotating the array so that the planet signal would be modulated through the fringe pattern at a predictable frequency.

Bracewell originally envisaged a rotating two-element interferometer on a rigid structure. Subsequent studies have pointed out that greatly improved sensitivity would be possible using four or more elements with adjustable sep-

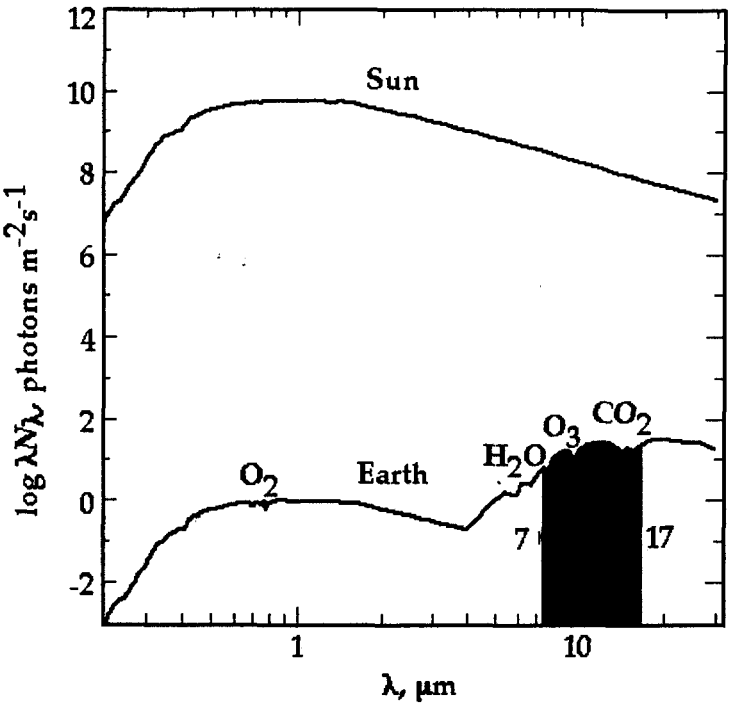

Figure 1. The spectral energy distributions of the Sun and the Earth as seen from 10 pc away demonstrate that the contrast ratio problem, while severe in the mid-infrared, is a factor of 1,000 times more favorable than at visible wavelengths. Additionally, the mid-infrared region contains a number of strong, broad spectral features of trace atmospheric gases.

arations (Angel 1990; Leger et al . 1996; the *ExNPS* report, 1996; Angel and Woolf 1997; see Shao and Colavita, 1992 and Woolf and Angel, 1998 for general reviews). The primary motivation for using more elements is to provide greater starlight suppression. The null should be as broad and deep as possible, but have an angular extent no larger than the orbit of the innermost planet. An interferometer array with more than two elements also offers the potential of fringe patterns with more complicated symmetry to help overcome ambiguities in the image reconstruction. Moreover, if the telescope separations are adjustable, as would be the case in a free-flyer configuration, the restrictions on the shape and width of the null could be relaxed, because the fringe pattern of the array could then be tuned to each candidate star. Mariotti and Mennessohn (1997) and Woolf et al. (1998) have emphasized the need for an additional level of signal modulation, a technique called "chopping," to suppress light arising from the extended zodiacal cloud around the star and to modulate the desired planetary signals in the face of varying backgrounds and detector drifts.

2. The TPF Interferometer

The Terrestrial Planet Finder (TPF) could be implemented in wide variety of configurations, constrained by the number of telescopes, the necessary degree of starlight and background suppression, and the required accuracy of the reconstructed images. There is a performance trade-off between the ability to provide a deep and wide null to suppress starlight combining many telescopes into a single array, and the ability to chop rapidly and to suppress large-scale diffuse emission from a zodiacal cloud by chopping between sub-arrays with relatively shallow nulls (Velusamy, Shao and Beichman, 1999, this conference).

2.1. Factors Affecting the Sensitivity of TPF

We now consider some of the high level details of TPF's design. An illustrative concept (Table 1) provides a reference for describing the various elements of TPF. It uses a linear array of four telescopes and can employ chopping or not depending on the configuration of the beam combiner.

Table 1. Interferometer Observing System

Baseline	75 m
Telescope Apertures	1.8:3.5:3.5:1.8 m (1AU) 1.1:2.2:2.2:1.1 m (5 AU)
Telescope Temperature	40 K(1 AU) 35 K(5 AU)
Telescope Emissivity	0.1
Optics temperature	10 K
Optics Emissivity	0.4
Spectral Resolution	20
Net Efficiency (Optics· Detector·Beam)	0.04
Deepest Null	10^{-5} (1 AU) 10^{-6} (5 AU)
Phase Center Pointing Jitter	0.25 milli-arcsec
Detector Dark Current	5 e^-/sec
Detector Read Noise	1 e^-
Flat Field Error	10^{-5} (1 AU) 10^{-4} (5 AU)

The sensitivity of TPF is determined by a wide variety of factors, some relating to the target system, some to the instrument, and some to the observing location. This section outlines some of the key tradeoffs and demonstrates that an interferometer using 3.5 m telescopes located at 1 AU can detect terrestrial planets in a few hours, characterize their habitability in a few days, and look for signs of photosynthetic life in a few weeks. Some of the essential astronomical and instrumental factors affecting the ability of TPF to meet its goals include:

- The size, temperature and atmospheric composition of the target planet.

- The distance to the stellar system, the luminosity and physical size of the star.
- The distribution and amount of material of the zodiacal dust in the target system.
- The inclination of the orbital plane to the line of sight.
- Observatory properties such as the size and temperature of the telescopes and associated optics, interferometer baseline and nulling configuration, pointing jitter, etc.
- Instrument properties such as optical efficiency, detector dark current, depth and stability of the null.
- Local background due to dust in the solar system at the observing location and in the direction of the target.

Each of these factors must be evaluated carefully to assess the realism of a particular design. Tables 1-3 list the parameters used in the simulations. The calculations summarized in Tables 4 and 5 lead to the following conclusions:

1. The emission from exo-zodiacal dust in the target solar system greatly reduces the influence of observing location on the performance of TPF. If emission from a solar system zodiacal cloud (1 Zody) fills a telescope beam, it doesn't matter whether that surface brightness arises locally within our solar system, or from the dust cloud surrounding the target star. For example, adding the photon noise produced by the exo-zodiacal signal from a 1 Zodi cloud increases the required collecting area of a 5 AU interferometer by *a factor of two* to make an observation to a particular sensitivity in a given time, e.g. from 1.5 m mirrors to 2.2 m mirrors. On the other hand, adding in the noise from a 1 Zodi cloud increases the required collecting area of a 1 AU system by only 20% (e.g, from 3.2 m to 3.5 m).
2. A four element interferometer using 3.5 m telescopes operating at 1 AU can achieve a signal to noise (SNR) of 7 on an Earth-like planet at 10 pc in 10^5 s of integration time at a spectral resolution R=20 (Table 5). This assumes the target system is surrounded by a 1 Zodi cloud.
3. Modest spectral resolution (R$\sim$20) can be used to characterize the atmospheres of detected planets in longer, but still credible integration times. A spectrum of R=20 at SNR=10, enough to detect CO_2 and H_2O, would take just 2.3 days. A SNR=25 spectrum at R=20 needed to detect O_3 would take 15 days.
4. Higher spectral resolution and sensitivity than are currently feasible would be required to detect *terrestrial* levels of other indicators of biological activity such as CH_4 or N_2O (R$\sim$1000). However, other ecosystems could have far different line strengths than terrestrial so the TPF design should not preclude the ability to find lines throughout the thermal IR spectrum.

Table 2. Properties of a Target Planet

Distance	10 pc
$R_{\rm planet}$	1 $R_\oplus$
$L_\star$	1 $L_\odot$
Orbital distance, a	1 AU
$T_{\rm planet}$(10 microns)	265 $a^{-0.5} L_\star^{0.25}$ K
F_ν(planet)	0.34 mJy @ 12 μm

The following paragraphs detail some of the most important factors that affect the capabilities of TPF. The first set are astrophysical concerns that can be ameliorated, if at all, only by target selection. The remainder are properties of the TPF instrument.

The Target Planet. The target planet is typically taken to be an Earth-diameter blackbody at an orbital radius a=1 AU around a solar type star at distance d=10 pc. Various atmospheric constituents can modify the appearance of the planet (Figure 1) and its effective temperature at a particular wavelength.

The Effects of Zodiacal Emission. The emission from zodiacal dust in our own solar system and in the target system is an important source of noise. In the absence of any other information, we adopt the fan-shaped form that characterizes our solar system dust for the structure of the exo-zodiacal cloud, varying only the scaling factor for the optical depth (ρ_0) to account for differing amounts of zodiacal material (Reach et al. 1994). Eqn.1 is used to evaluate the emission along any line of sight. The temperature structure varies according to the luminosity of and distance from the central star. Equation 2 gives the equilibrium temperature of a dust grain located r(AU) from its central star. (r, z) are cylindrical coordinates within the cloud:

$$\mathcal{I}_\nu = \int B_\nu(T(r))\rho_0 \; r^{-\alpha} e^{-\beta(z/r)^\gamma} d\ell \tag{1}$$

$$T(r) = T_0 r^{-\delta} \tag{2}$$

Local Zodiacal Cloud. The local zodiacal (LZ) cloud provides the foreground through which TPF must observe. The cloud is characterized by the zodiacal parameters described in Table 3 where the parameter values are derived from fits to the COBE or IRAS data (Reach et al. 1995). The LZ diminishes with distance from the Sun due to decreased dust density and decreased temperature. At short wavelengths the drop is very dramatic (a factor of >300 at λ <7 μm) while at longer wavelengths the drop is less pronounced (~150 at 12μm).

Infrared Cirrus. An additional background against which TPF must observe is the galactic cirrus, which sets a minimum sky brightness even if there were no LZ emission (Bernard et al. 1992). A minimum value of the cirrus emission corresponding to $\mathcal{I}_\nu(100\mu m)$ = 1 MJy/sr is included in all calculations, e.g., $\mathcal{I}_\nu$(12 μm) ~0.08 MJy/sr from cirrus.

Table 3. Properties of Zodiacal Cloud

ρ_0	1.14×10^{-9} AU^{-1}
α	1.39
β	3.26
γ	1.02
Temperature at 1 AU (T_0)	$286(L/L_0)^{0.25}$
δ	0.42
Local Zodiacal surface brightness at 30° inclination at 12 μm	19 MJy/sr (@1 AU) 0.23 MJy/sr (@5 AU, including cirrus)
Dust destruction temperature	1500 K

Exo-Zodiacal Emission. The exo-zodiacal cloud contributes photon noise to the total signal starting at the dust sublimation radius and extending out to the edge of the primary beam of a single telescope. A two-dimensional image of the zodiacal cloud is determined by integrating the 3-dimensional dust distribution (Eqns. 1 and 2) for a particular inclination to the line of sight. Since the signal reaching the detector passes through the null pattern of the interferometer, the hot, inner portions of the zodiacal disk are hidden from view and the Poisson-noise producing zodiacal signal is decreased by about a factor of ~3 from the nominal exo-zodiacal flux.

Structured EZ Component. Structured emission in the zodiacal light of the target star is potentially a noise source. A planet must be detected against a non-flat field of corrugations in the target field. Structures in our own cloud have roughly <0.1% of the amplitude of the total cloud brightness (as discussed at Exozodiacal Dust Workshop; Backman et al. 1998). At levels less than 1% of the total brightness, the structured emission is not a significant contributor to the noise budget. However, large coherent structures, such as wakes and clumps behind planets, can masquerade as planets or serve as markers for their presence.

Background Confusion Noise. Extrapolation of 12 μm star and galaxy counts indicate that confusion noise will not be an issue at the high spatial resolution of TPF.

Interferometer Properties. The interferometer taken as a reference system for this study has properties listed in Table 1. The Oases system (Angel and Woolf 1996) is but one of many possible nulling configurations in which light from pairs of telescopes are combined (nulled) and then pairs of interferometers are combined for a still higher order of rejection. The separation between the telescopes and the amplitudes of the signals from the telescopes are matched to produce a particular null. The Oases system utilizes a ratio of telescope diameters of 1:2:2:1 or 1:3:3:1 to give a deep null (10^{-6}) suitable for operation in low background conditions. The breadth of the Oases null ($\propto \theta^6$) is suitable for fixed baselines that cannot be tuned for stars at different distances.

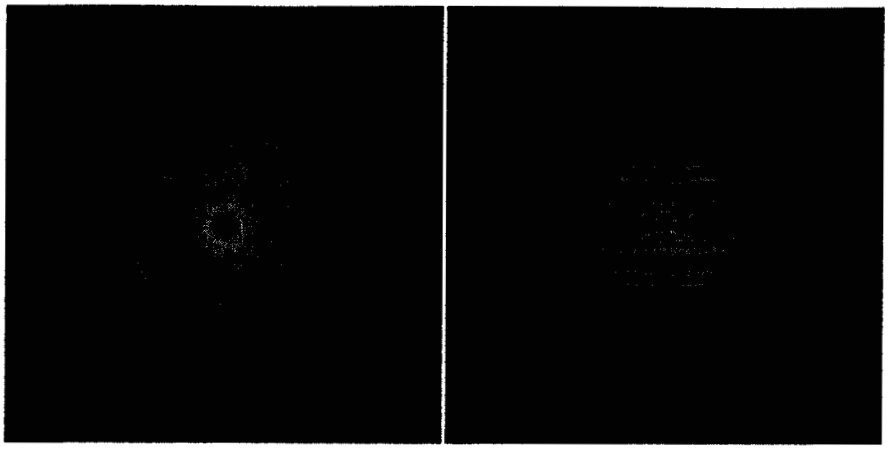

Figure 2. A simulated zodiacal dust disk with (right) and without (left) the TPF fringe pattern superimposed on it. The signal detected by TPF is the integral of all the light passing through the fringe pattern. The fringe pattern rotates as TPF rotates around the line of sight to the target star, thereby modulating the signal from a planet. The star, located at the center of the fringe pattern, remains nulled at all times.

The interferometer projects a nulling interference pattern onto the sky. Let $\Theta(r,\theta)$ be the fringe pattern of the interferometer, where *theta* is the orientation of the fringe pattern on the sky and r is the radial distance from the center (Figure 2). The nulling pattern for the 4-telescope Oases interferometer arranged in a 1:2:2:1 configuration and overall dimension B is given by

$$\Theta(r,\theta) = 4\sin^2\phi\sin^4(\phi/2) \qquad \text{with} \qquad \phi = 2\pi r\cos\theta(0.5B)/\lambda \tag{3}$$

A perfect interferometer would produce fringes with perfect contrast. We clip the null to have a maximum depth of 10^{-6} for the 5 AU system at 10^{-5} for the 1 AU system. At the closer distance, the higher local background relaxes the requirements for the deepest possible null. As described below, some interferometer configurations allow for rapid chopping of the nulled signal to enhance detectability of a planetary signal in the presence of various detector or thermal drifts.

Leakage Signal. The amount of star light coming through the null is given by

$$Q_{\text{leak}} = A_{\text{tel}}N_{\text{tel}}\frac{\Delta\nu\eta\tau}{h\nu}\int\int B_\nu(r,\theta)\Theta(r,\theta)r\,dr\,d\theta \tag{4}$$

integrated over the stellar radius. $A_{\text{tel}}N_{\text{tel}}$ is the total collecting area, corrected for the reduced signals from the outer telescopes in the 1:2:2:1 or 1:3:3:1 configurations. $\Delta\nu$ is the bandwidth of the observation; h is the product of the optical detector quantum and beam efficiencies; τ is the integration time; and $h\nu$ is the quantum of energy at the observing frequency, ν.

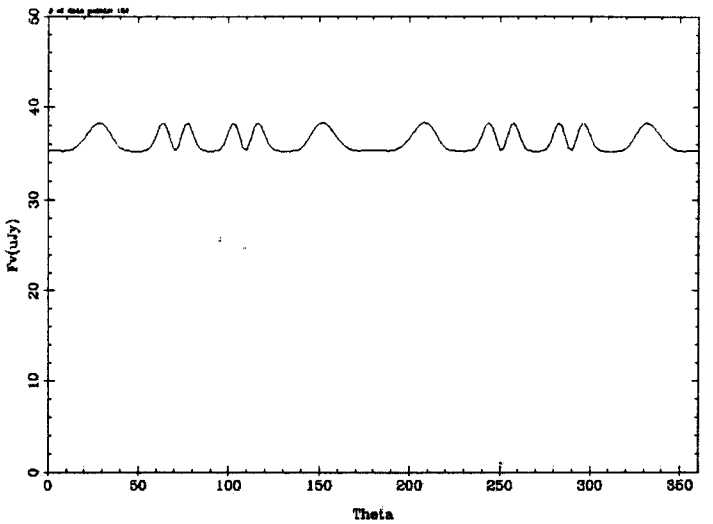

Figure 3. Figure 3. As TPF rotates around the line of sight to a target star, the planet (a $3R_{\oplus}$ planet is shown for clarity) produces a modulated signal as it moves in and out of the interferometer fringe pattern. TPF would produce ~20 such data streams, one for each of the observed wavelengths, that would be combined to reconstruct an image of the solar system and the spectra of any detected planets.

Leakage Jitter. An additional noise source comes from wandering of the null across the star due to variations in pointing of the phase center of the interferometer. As the phase center of the starlight drifts within the null pattern, the amount of leakage varies. Calculations show that the noise associated with this jitter is negligible for values < 1 milliarcsec. This noise source depends on the angular diameter of the star, the breadth of the null, and the stability of the system. In practice, the interferometer will be stabilized at 2 μu where 1 milliarcsec corresponds to 1/100 of the point spread function and typically to 1/10 of a fringe spacing. The high signal-to-noise ratio expected from target stars (>1000:1 in a few milliseconds) is consistent with this stability requirement.

Telescope Properties. The telescope and optics temperatures are set by the need to avoid any contribution to instrumental noise by the telescope. The temperature depends on the wavelength and local zodiacal foreground. At 1 AU a telescope temperature of 40 K produces <10% degradation of the sensitivity at 17 μm. At 5 AU, the telescope temperature must be < 35 K to avoid influencing the 17 μm sensitivity. The overall system efficiency includes reflections off many optical surfaces, transmission through filters and beamsplitters (0.12), detector quantum efficiency (0.5), and beam efficiency due to taking only the central part the primary beam (0.6). For operation at 1 AU and at low (R~20) spectral resolution, SIRTF detector performance is adequate. Detector properties expected as part of the development of NGST may allow increases in spectral resolution without incurring a read-noise penalty.

Signal to Noise Calculations. The signal detected by TPF depends on the location of the planet relative to position of the interferometer pattern projected onto the sky. The planet signal is modulated by the fringe pattern as the interferometer rotates around the line of sight to the star (Figure 2, 3). The total signal from the various sources of radiation (Figure 4) are defined as follows in terms of photo-electrons detected by TPF in an integration time, τ.

$$Q_{\rm planet}(r,\theta) = \Theta(r,\theta) B_\nu(\nu, T_{\rm planet}) \Omega_{\rm planet} A_{\rm tel} N_{\rm tel} \frac{\Delta\nu\eta\tau}{h\nu} \tag{5}$$

where $\Omega_{\rm planet}$ is the solid angle subtended by the planet.

The background signals come from the local, $Q_{\rm LZ}$, and exo-zodiacal, $Q_{\rm EZ}$, dust clouds.

$$Q_{\rm LZ} = A_{\rm tel} N_{\rm tel} \frac{\Delta\nu\eta\tau}{h\nu} I_\nu(LZ) \int\int \Theta(r,\theta) r dr d\theta \tag{6}$$

where the integral extends to the edge of the primary telescope beam, $r_{\rm max} = 0.66\lambda/D$. This choice of rmax optimizes the signal to noise for a background-limited measurement of a point source. Similarly, for the exo-zodiacal emission:

$$Q_{\rm EZ} = A_{\rm tel} N_{\rm tel} \frac{\Delta\nu\eta\tau}{h\nu} \int\int I_\nu(r,\theta) \Theta(r,\theta) r dr d\theta \tag{7}$$

The minimum level of noise arising from these photo-electrons is equal to the square root of the counts, $Q_{\rm tot} = Q_{\rm LZ} + Q_{\rm EZ} + Q_{\rm planet} + Q_{\rm dark}$. Another source of noise comes from instabilities in the observing system in the presence of large background signals. This "flat field" noise can be modeled as being linearly proportional to the total signal, $flat \cdot Q_{\rm tot}$, and represents a systematic noise level that cannot be improved with further integration time. Ground-based infrared systems typically operate at $10^{-6} - 10^{-7}$ of the large atmospheric background using rapid chopping (~30 Hz). Space systems typically operate at $10^{-3} - 10^{-4}$ of the low space background with no or only slow (<1 Hz) chopping. The requirements on background cancellation are quite different for the 1 AU case where the local zodiacal background is relatively high. Chopping may be required to make the system work at 10^{-5} of the background at 1 AU.

Detector Noise. Detector properties are given by the read noise, RN, and dark current, $Q_{\rm dark} = i_{\rm dark} \cdot \tau$. Linearity and stability must be optimized for a 1 AU system operating in the relatively high local background. Chopping at ~1 Hz is possible without noise penalty for devices with RN<10 e^-.

Total Noise. The total noise is the quadratic sum of all the individual components:

$$Q_{\rm noise} = \left[Q_{\rm leak} + Q_{\rm LZ} + Q_{\rm EZ} + RN^2 + Q_{\rm dark} + Q_{\rm planet} + (flat \cdot Q_{\rm tot})^2 \right]^{\frac{1}{2}} \tag{8}$$

which is to be compared with the exo-planet signal given in Eqn. (4) to give

$$SNR = Q_{\rm planet} / Q_{\rm noise} \tag{9}$$

Table 4 compares the noise and signals for the 1 and 5 AU systems described in Table 1 for a wavelength of 12 μm. The 1 AU system imposes less

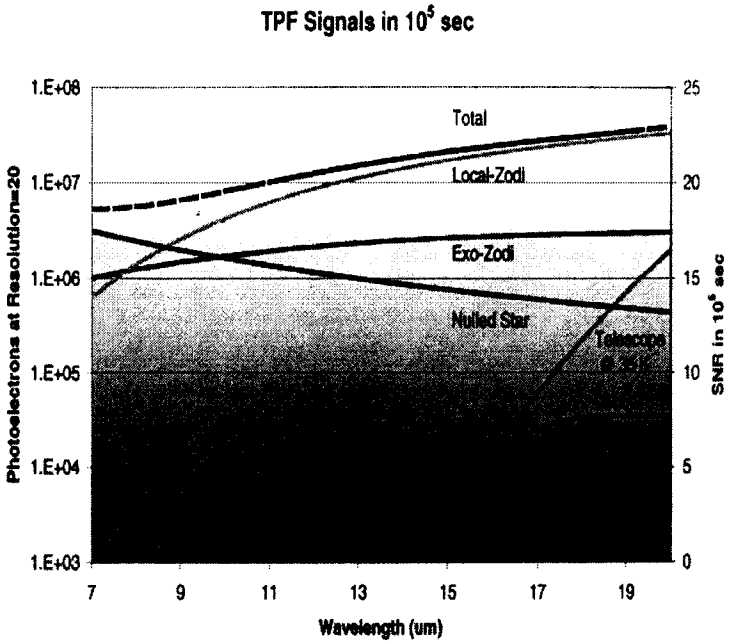

Figure 4. The signal in photo-electrons in a 10^5 sec integration period from an Earth-like planet observed through the (1 AU, 3.5m) version of TPF. The planet shows CO_2 absorption at 16 μm. The spectral resolution is R=20 and other parameters are as given in Table 1. Also shown are the other signals that contribute to the total photon shot noise. The bottom curve shows the SNR on the planet using the right-hand scale.

Table 4. Signal and Noise Sources at 1 and 5 AU

Signal (photo-electrons) R=5, $\tau = 10^5$ sec @ 12 μm	2 m (5 AU)	3.5 m (1 AU)
Planet @ 10 pc	0.008×10^6	0.025×10^6
Exo-Zodiacal Background	0.71×10^6	2.15×10^6
Local Zodiacal Background	0.10×10^6	8.56×10^6
Nulled Star Leakage	0.04×10^6	1.16×10^6
Dark Current	0.50×10^6	0.50×10^6
Total Counts	1.35×10^6	12.4×10^6
$\sqrt{(\text{Counts})}$	1.16×10^3	3.52×10^3
Flat·Counts	0.14×10^3	0.12×10^3
Noise	1.17×10^3	3.52×10^3
SNR (Signal/Noise)	7.0	7.1

stringent requirements on detector and nulling performance, as well as easier implementation and operational constraints. The two accomplish roughly the same sensitivity although with a very different balance of backgrounds, signal levels, and star leakage. Figure 4 compares the planetary signal (including CO_2 absorption) with the various sources of noise as a function of wavelength.

Table 5. Observing Time Requirements For Various Configurations of TPF to Observe Terrestrial Planets

Science Goal	12 μm observation of an Earth at 10 pc	4×2 m (5 AU)	4×0.85 m (1 AU)	4×2 m (1 AU)	4×2.7 m (1 AU)	4×3.5 m (1 AU)
Detect Planet	Spectral Resolution (R)=3 Signal to Noise (SNR)=5	1.4 hr	470 hr	15.3 hr	5.1 hr	2.0 hr
Detect Atmosphere CO_2, H_2O	R=20 SNR=10	2.4 day	–	18.1 day	5.9 day	2.3 day
Habitable? Life? O_3,CH_4	R=20 SNR=25	15.0 day	–	- -	–	14.7 day

Table 5 compares a broader range of possible interferometers. While a system consisting of SIRTF-style 0.85 m mirrors could barely detect planets at 10 pc, it could detect 1-2$R_\oplus$ planets at 5-8 pc in a few hours to a few days. A 1 AU system consisting of 2.7 m NGST mirror segments could detect broadband emission from an Earth at 10 pc in ~6 hours and even offer simple characterization of CO_2 and H_2O in a week. Such a system is a possible fallback if the baseline 3.5 m system cannot be achieved at reasonable cost.

2.2. Simulations of TPF Nulling.

Images of planetary systems are not formed by direct-imaging, but are reconstructed after measurements have been made with the array in multiple configurations. The array is rotated around the line of sight to the star with measurements made at successive position angles. The data consist of a time series of the planet's signal as it rises and falls through the fringe pattern of the rotating array (Figure 3). The process can be repeated with the telescopes at different separations as well. Despite the lack of complex phase information, these data, obtained simultaneously at ~20 wavelengths, can be turned into an image using a number of numerical techniques including a cross-correlation method (Angel and Woolf 1997) or a maximum correlation method (Aumann et al. 1990; Beichman and Velusamy 1997) analogous to the Fourier transform approach used in synthesis imaging.

We used the Maximum Correlation Method (MCM) to investigate the ability to find a planet in presence of differing amounts of zodiacal dust, inclination angles, and observing strategies. The MCM technique iteratively fits a model image as observed through the TPF observing system, e.g. with the beam pro-

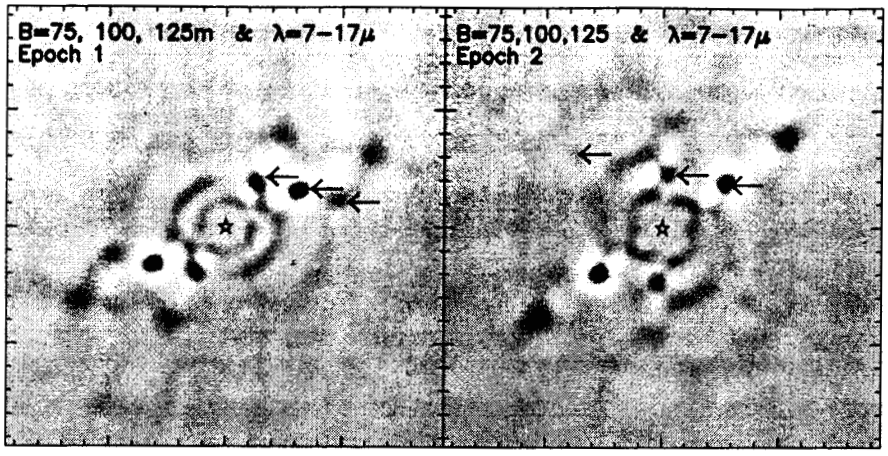

Figure 5. A reconstruction of a planetary system at 10 pc containing Venus, Earth, and Mars at two epochs.

file described by Eqn.(3), to the observed time series in a way that is consistent with the data and its associated noise. Figure 5 shows a reconstruction of a TPF image for system consisting of Venus, Earth, and Mars as viewed from 10 pc away at an inclination angle of 30 deg. Venus and Earth are quite prominent, while Mars is below the threshold of detection. The reconstruction shows a few artifacts such as echoes of each planet on the opposite side of the star and at twice the orbital distance. These artifacts can be removed with more sophisticated data acquisition (chopping) and image processing strategies.

3. A Program for Planet Finding.

TPF will detect and characterize planets around nearby stars in three stages spread throughout TPF's five year mission:

- Perform a survey of ~150 stars looking for planets (terrestrial and larger) around a large variety of stars.
- Carry out spectroscopic follow-up observations of ~50 systems looking for broad, strong spectral lines of species such as CO_2 and H_2O.
- Make very sensitive spectroscopic observations of ~5 most favorable systems looking for O_3.

The sensitivity of TPF as described above is adequate to carry out this program and to leave between 30-50% of the time available for general purpose astrophysical imaging.

4. Relationship of TPF to Other NASA Missions

Missions presently in the NASA program will provide the foundation of scientific knowledge and technological skills needed for TPF (Table 6). These projects

include the Keck Interferometer, the Space Interferometer Mission (SIM), the Next Generation Space Telescope (NGST) and the Space Technology-3 mission. With these projects completed NASA, perhaps in conjunction with other space agencies, will be ready to start TPF.

5. Conclusion

Table 6. Scientific and Technological Precursors to TPF

Project	Science	Technology
Ground-based Interferometers: Keck Interferometer Large Binocular Telescope (LBT) Very Large Telescope (VLTI)	Exo-zodiacal emission Planet census	Interferometry hardware & software Nulling Community training
Space Infrared Telescope Facility (SIRTF)	Exo-zodiacal emission Planetary companions	Passive cooling Drift away orbit IR detectors
Deep Space 3 (DS-3)	–	Formation Flying Interferometer Operations
Space Interferometry Mission (SIM)	Planet census Exo-zodiacal emission	Interferometry hardware, software, operations Nulling
Next Generation Space Telescope (NGST)	Exo-zodiacal emission Planetary companions	Lightweight optics Cryogenic actuators Active coolers

The Terrestrial Planet Finder will not be an end-point of the Origins program. If TPF succeeds in identifying oxygen-bearing planets around nearby stars, a natural follow-on mission would be the "Life Finder" which would operate in manner similar to TPF, but at the much higher spectral resolution needed to identify rare trace gases such as CH_4 or N_2O that are unambiguous markers of life when found in conjunction with gases like H_2O and O_3. Such a system would require ~25 m apertures instead of TPF's 3.5 m telescopes. Beyond "Life Finder", one can envision a "Planet Imager" that would make resolved images of distant planets. We have only the barest conception of how one might design such a system (see chapter 14 of the TPF Report 1999; Labyerie, 1999, this conference), but we know it will require hundreds or thousands of square meters of collecting area spread out over hundreds (visible light) or thousands (infrared) of kilometers. Thus, TPF will be a vital way-station in humanity's long quest to discover the origins of life, to learn whether or not the Universe teems with life, and ultimately to deepen and broaden our understanding of ourselves and of our place in the Universe.

Acknowledgments. This work was funded by NASA. JPL is operated for NASA by the California Institute of Technology under a contract with Caltech. We would like to acknowledge the assistance of John Fowler in adapting the MCM algorithm for use in these simulations.

References

A Road Map for the Exploration of Neighboring Planetary Systems ("The ExNPS Report") 1996, edited by C. A. Beichman (JPL: Pasadena), JPL 96-22.

Angel, J.R.P. 1990, The Next Generation Space Telescope, Bely, P. and Burrows, C.J., TPF: The Terrestrial Planet Finder, eds. Beichman, C.A. Woolf, N.J., and Lindensmith, C. 1999.

Illingworth, G. eds. (STScI: Baltimore), p. 81.

Angel, J. R. P. and Woolf, N. J. 1997, Ap.J. 475, 373.

Aumann, H. H., Fowler, John W., Melnyk, M. 1990, Astr. J., 99, 1674.

Backman, D. E., Caroff, L. J., Sanford, S.A., Wooden, D.H., Proceedings of the Exozodiacal Dust Workshop, 1997, NASA/CP–1998-10155.

Beichman, C.A. and Velusamy, T. 1997, Bull. Am. Astr. Soc., 29, paper 64.03.

Bernard, J. P., Boulanger, F., Desert, F. X., Puget, J. L. 1992, A&A, 263, 258.

Bracewell, R.N., Macphie, R.H.1979, Icarus, 38, 136.

Labyerie, A., 1999, this conference. Leger, A., Mariotti, J. M., Mennesson, B., Ollivier, M., Puget, J. L., Rouan, D., Schneider, J. 1996, Icarus, 123, 249.

Mariotti, J-M. and Mennessohn, B. 1997, internal ESA report for the IRSI project. Reach et al. 1995, Nature, 374, 521.

Shao, M. and Colavita, M. M. 1992, Ann. Rev. Astron. Astrop. 30, 457.

Velusamy, T., Shao, M. and Beichman, C.A., 1999, this conference.

Woolf, N. J. and Angel, J.R. 1988, Ann. Rev. Astron. Astrop. 36, 507.

Woolf, N. J. et al. 1998, Proc. SPIE 3350 on Astronomical Interferometry, R.D. Reasenberg ed. 683.

Discussion

Ed Shaya: As we progress to larger and larger interferometers the cost of lifting them off the ground will become prohibitive. Have there been studies of the trade-offs of moon-based versus free-flying interferometers for these very large instruments?

Charles Beichman: People have looked at the moon as a base for astronomy. The major conclusion we came to was that if society makes a major investment in a lunar base, then astronomy could take the advantage of it. But without that commitment, astronomy is better carried out in space.